Effects of epidemiological structure on the transient evolution of HIV virulence

Sang Woo Park and Ben Bolker

April 1, 2016

1 Introduction

How pathogen virulence evolves is a fundamental question in evolutionary biology, of both theoretical and (potentially) practical importance. The trade-off theory (Ebert, 1999) — which postulates that parasite virulence can be explained as the long-term evolutionary outcome of a saturating relationship between parasite clearance rate and transmission rate — has been criticized (Ebert and Bull, 2003; Alizon and Michalakis, 2015), but has also been successfully applied in several important cases (Dwyer et al., 1990) . One particularly interesting application of these ideas is the work by Fraser et al. showing that HIV appears to satisfy the prerequisites of the tradeoff theory: in a study of discordant couples (i.e. long-term sexual partnerships with one infected and one uninfected partner), HIV virulence as measured by the rate of progression to AIDS was both heritable and covaried with the set-point viral load (i.e., the characteristic virus load measured in blood during the intermediate stage of infection), which in turn predicted the probability of within-couple transmission (Fraser et al., 2007, 2014). Subsequent studies (Shirreff et al., 2011; Herbeck et al., 2014) used these data to parameterize mechanistic models of HIV virulence evolution, suggesting that HIV invading a novel population would initially evolve increased virulence, peaking after approximately [XXX] years and then declining slightly to a long-stable virulence level.

The work of Shirreff et al., and particularly the predicted transient peak in HIV virulence midway through the epidemic, highlights the importance of interactions between epidemiological and evolutionary factors (Day and Proulx, 2004; Alizon, 2009). However, despite the attention to mechanistic detail at the individual or physiological level, the epidemiological structures used in these models are relatively simple. As we discuss in detail below, the existing models of HIV eco-evolutionary dynamics either use implicit models that incorporate the average effects of within-couple sexual contact — without representing the explicit dynamics of pair formation and dissolution or accounting for extra-partnership contact — or use an agent-based formulation with parameters that effectively lead to random mixing among infected and uninfected individuals.

others? de Roode and Altizer?

read/check fraser+ 2014!; check vs. Herbeck et al. (2012)

don't forget to check other recent papers: esp Payne et al. (2014)

Here we explore the effects of incorporating *explicit* epidemiological structure in eco-evolutionary models.

We add complexity to the epidemiological model following the general approach of Champredon et al. (2013); individuals join and leave partnerships at a specified rate, and can have sexual contact both within and outside of established partnerships. At the same time, our analysis somewhat simplifies the models of Shirreff et al., for computational tractability; we check that our qualitative results are not sensitive to these simplifications. In order to explore how virulence evolution depends on epidemiological structure, we consider a series of models with increasing levels of complexity. In order to avoid dependence of the results on a particular set of parameters — as we explain below, finding matching sets of parameters across models with widely differing epidemiological structures is challenging — we evaluate our models across a wide range of parameters, again following Champredon et al. in using a Latin hypercube design. For each model run, we compute a set of metrics (peak virulence, timing of virulence peak, equilibrium virulence) that summarize the evolutionary trajectory of a simulated HIV epidemic.

2 Methods

2.1 Model formulation

As our primary goal is to explore how different epidemiological structures (i.e. partnership dynamics and contact structures) affect our conclusions about the evolution of virulence, our models use a simplified description of within-host dynamics and heritability derived from Shirreff et al.'s multi-strain evolutionary model. Like Shirreff et al., we use a simple susceptible-infected-susceptible demographic formulation; rather than modeling birth and death (or more specifically, recruitment into the sexually active population and death), we assume that whenever an individual dies from infection, another enters the susceptible compartment.

2.1.1 Infection dynamics

was going to call this "within-host" but it includes transmission

Like Shirreff et al., we focus on the evolution of mean $\log_{10}$ set-point viral load, SPVL (which we denote as α), rather than virulence (i.e. rate of progression to AIDS) itself. In contrast to Shirreff et al., we use a single-stage disease model instead of accounting explicitly for progression through the three main stages of HIV infection (primary, asymptomatic, and disease), and we use a simple exponentially distributed infectious period instead of a more realistic Weibull-distributed infectious period. We account for varying transmission rates and durations of each disease stage by summing the durations of three stages (again based on Shirreff et al.'s model) and taking the duration-weighted average of transmission rates of three stages. Thus the within-couple transmis-

sion rate, β, for our models is given by:

$$\beta(\alpha) = \frac{D_P\beta_P + D_A(\alpha)\beta_A(\alpha) + D_D\beta_D}{D_P + D_A(\alpha) + D_D} \tag{1}$$

where the duration of infection (D_P and D_D) and rate of transmission (β_P and β_D) of the **P**rimary and **D**isease stages of infection are independent of the host's SPVL. Following Shirreff et al., the duration of infection (D_A) and rate of transmission (β_A) for the **A**symptomatic stage are Hill functions of the SPVL:

$$\begin{aligned} D_A(\alpha) &= \frac{D_{\max} D_{50}^{D_k}}{V_\alpha^{D_k} + D_{50}^{D_k}}, \\ \beta_A(\alpha) &= \frac{\beta_{\max} V_\alpha^{\beta_k}}{V_\alpha^{\beta_k} + \beta_{50}^{\beta_k}}, \end{aligned} \tag{2}$$

where $V_\alpha = 10^\alpha$. The **u**ncoupled and **e**xtra-couple transmission rates are scaled by multiplying the **w**ithin-couple transmission rate β by the contact ratios c_u/c_w and c_e/c_w.

2.1.2 Mutation

Like Shirreff et al. we incorporate a between-host mutation process in the SPVL, but simplify Shirreff et al.'s evolutionary model slightly by using a one-to-one genotype-phenotype mapping. The mutational process in our model is directly taken from Shirreff et al.. Over the course of infection, mutation occurs within the host. However, it is assumed that SPVL of an infected individual is determined by the SPVL at the time of infection for simplicity (and is not further affected by within-host mutation). Instead, the mutational effect takes place when an infected individual transmits the virus to a susceptible individual. First, the distribution of $\log_{10}$ SPVL is discretized into a vector:

$$\alpha_i = (\alpha_{\max} - \alpha_{\min})\frac{(i-1)}{n-1} + \alpha_{\min} \qquad i = 1, 2, 3, \ldots n. \tag{3}$$

Then, we construct a mutational matrix, M — which is multiplied with the transmission term — so that M_{ij} is the probability that a newly infected individual will have $\log_{10}$ SPVL of j given that the infector has $\log_{10}$ of i. Finally, the probabilities are normalized so that each row sums to 1:

$$M_{ij} = \frac{\Phi(\alpha_j + d/2) - \Phi(\alpha_j - d/2)}{\Phi(\alpha_{max} + d/2) - \Phi(\alpha_{min} - d/2)}, \tag{4}$$

where $\Phi(j)$ is the Gaussian cumulative distribution function with mean α_i and variance of σ_M^2, and $d = (\alpha_{\max} - \alpha_{\min})/n$. Transmission rate and disease induced mortality rates are discretized into a vector as well:

$$\begin{aligned} \beta_i &= \beta(\alpha_i) \\ \lambda_i &= \frac{1}{D_P + D_A(\alpha_i) + D_D} \end{aligned} \tag{5}$$

2.1.3 Contact structure and partnership dynamics

We developed six multi-strain evolutionary models, designed to cover a gamut between Champredon et al.'s relatively realistic and Shirreff et al.'s relatively simplistic epidemiological structures, each of which is based on different assumptions regarding contact structure and partnership dynamics. Specifically, we focus on the effects of the assumptions of (1) instantaneous vs. non-instantaneous partnership formation and (2) zero vs. positive extra-partnership sexual contact and transmission on the evolution of mean $\log_{10}$ SPVL.

Our first four models consider explicit partnership dynamics and are based on Champredon et al.'s model. Model 1 and 2 assume non-instantaneous partnership formation (i.e. individuals spend some time uncoupled, outside of partnerships) and consist of five states that are classified by infection status and partnership status. S is the number of single (uncoupled) susceptible individuals, and I is the number of single infected individuals. SS is the number of susceptible-susceptible couples, SI is the number of serodiscordant (susceptible-infected) couples, and II is the number of concordant positive (infected-infected) couples. Model 1 includes extra-partnership contact (with both uncoupled individuals and individuals in other partnerships) whereas model 2 only considers within-couple transmission. Models 3 and 4 assume instantaneous partnership formation and thus consist of only the three partnered states: SS, SI, and II. Parallel to model 1 and 2, model 3 includes extra-partnership contact (now only with individuals in other partnerships, since uncoupled individuals don't exist in this model) and model 4 only considers within-couple transmission.

In contrast, models 5 and 6 are not explicitly structured. Model 5 is an implicit serial monogamy model based on the epidemiological model used by Shirreff et al.. It is actually a random mixing model that consist of only two states, S and I, and does not consider explicit partnership dynamics. However, to simulate the effect of instantaneous partnership formation, it uses an adjusted transmission rate that is derived from approximated basic reproduction number of a serial monogamy model Hollingsworth et al. (2008) . Finally, model 6 is a simple random-mixing model.

is this the right ref? where does Shirreff's model originate?

I think we need a section here to describe partnership dynamics/contact structure, i.e. define the ρ, c_u, c_e, c_w parameters - will be similar to Champredon et al.

2.2 Latin hypercube sampling

Despite considerable effort by many researchers (e.g. Hollingsworth et al., 2008; Champredon et al., 2013), the parameters determining the rate and structure of sexual partnership change and contact are still very uncertain; this led Champredon et al. to adopt a Latin hypercube sampling (LHS) strategy (Blower et al., 1991) that evaluates model outcomes over a range of parameter values. In order to make sure that our comparisons among models apply across the entire space of reasonable parameter values, and in order to evaluate the differential sensitivity of different model structures to parameter values, we follow a similar protocol and perform LHS over a parameter set including both the transmission and duration parameters (β_P, D_P, β_D, D_D) and contact/partnership

parameters (ρ, c, c_u/c_w, and c_e/c_w). We do not allow for uncertainties in parameters that are directly related to evolutionary process

i.e., ... ?

Latin hypercube sampling is done as in Champredon et al.. For each parameter, z, its range is divided into N equal intervals on a log scale, where N is the number of total runs:

give the number we actually used here

$$z_i = \exp(\log(z_{min}) + [\log(z_{max}) - \log(z_{min})]\frac{i-1}{N-1}) \qquad i = 1, ..., N. \quad (6)$$

For simplicity, we assume that all parameters follow logarithmic distribution. Following the vectorization of a parameter range, a matrix is constructed so that each column contains a vector of a parameter series which it represents (z_1,...z_N). Then, each column is replaced with a random permutation series of itself. Now, each row contains a different parameter set that is used for each simulation run.

Table 1 gives the ranges of the model parameters used for LHS. Parameters ranges regarding contact and partnership dynamics (ρ, c, and c_e/c_w) are taken from Champredon et al., whereas those regarding infection (β_P, D_P, β_D, and D_D) are taken from Hollingsworth et al. (2008). Rest of the parameters are taken from Shirreff et al..

As we introduce a new parameter, c_u/c_w, to model uncoupled and extra-couple transmission dynamics more easily within multi-strain models (refer to appendix), it is important to pick a reasonable range for it. Champredon et al.assume that the effective within-couple contact rate and effective uncoupled contact rate have the same range of 0.05 - 0.25. Given Champredon et al.'s parameter range, it is trivial that the possible maximum and minimum values of c_u/c_w are 5 and 1/5. Therefore, we use 1/5-5 as the range for the parameter c_u/c_w. Although this adds more uncertainty to the parameter c_u — Champredon et al.'s range gives 5 fold difference whereas ours give 25 fold difference — as there is not much known about the uncoupled transmission rate, it is reasonable to use a wider range.

refer to Table 1 and describe where the new parameters come from; e.g. decisions we made about new scaling parameters

2.3 Simulation runs

One of the most difficult parts of model comparison is finding parameter sets that are commensurate against many different model structures. For the most part, our models are too complex to easily derive analytical correspondences among them. Given a numerical criterion, such as r (initial exponential growth rate) or $\mathcal{R}_0$ (intrinsic reproductive number), we can adjust one or more parameters by brute force to ensure that all of the models match according to that criterion. While $\mathcal{R}_0$ is often considered the most fundamental property of an epidemic, and might thus seem to be a natural goal, here we focus on matching the initial growth rate r for several reasons. First, our primary interest is in the transient evolutionary dynamics of virulence, which are more strongly affected by r than $\mathcal{R}_0$ (CITE?). Second, r is in general more directly observable

in real epidemics; r can be estimated by simply fitting an exponential curve to the initial incidence or prevalence curves (CITE Ma et al.), while $\mathcal{R}_0$ typically requires either (1) knowledge of *all* epidemic parameters or (2) relatively sophisticated back-calculation based on r and knowledge of the serial interval or generation interval of the disease (CITE Wallinga, Teunis, Lipsitch, etc.) Thus, we scale a parameter so that every run has an equal exponential rate of growth rate.

In order to allow for all models to have equal initial exponential growth rate, r, we need to pick a parameter, s, so that $\lim_{s\to 0} r(s) = 0$ and $\lim_{s\to\infty} r(s) = \infty$. As adjusting either partnership change rate (i.e. partnership formation and dissolution rate) or transmission rate does not fulfill this requirement for certain models, we decided to scale partnership change rate and dissolution rate by the same factor of γ: $\beta_{\text{adj}} = \gamma\beta_{\text{base}}$, $c_{\text{adj}} = \gamma c_{\text{base}}$, $\rho_{\text{adj}} = \gamma\rho_{\text{base}}$. Since transmission rate is adjusted by the scale of γ, uncoupled and extra-couple transmission rates are adjusted as well. For model 3, 4, and 5, all of which assume instantaneous partnership, only the transmission rate and partnership dissolution rate are adjusted.

We run each model for 1000 times with different parameter sets calculated from Latin hypercube sampling [CITE Blower et al], with fixed starting conditions of mean $\log_{10}$ SPVL of 3 and epidemic size of 10^{-4} (refer to appendix). An initial run of After each run, initial exponential growth rate is calculated. Then, parameters are scaled so that the initial exponential growth rate is scaled to 0.04, which is approximately equal to that of Shirreff et al's model.

mention that baseline parameters are geometric means of ranges

For each model we derive the following summary statistics: peak virulence, peak time, equilibrium virulence, and relative peak virulence. The transient phase of an epidemic is often characterized by high virulence, and we define peak virulence as the maximum virulence during this phase. It is simply calculated by taking the maximum value from the virulence trajectory, and peak time is the time at which the maximum value is reached. Once the epidemic enters the endemic phase, evolution of virulence stabilizes and reaches equilibrium. Equilibrium virulence is calculated by taking the mean virulence at 4000 years. Although most simulations reach equilibrium much earlier, we set our time horizon at a much later date as some simulation runs have slow rate of evolution depending on the parameter set and model assumptions.

Do we need to talk about the baseline parameters? We never use it... We only use it for the first set of graphs but we need to mention that we are using Shirreff's partnership rate just for comparison...So we actually never use baseline parameters...

We focus on these statistics for the following two reasons. First of all, knowing the possible ranges for the peak virulence allows us to estimate the worst-case scenario for the HIV and other sexually transmitted disease epidemics. When an epidemic begins, it is often the case that the pathogen has already evolved towards high virulence by the time it is observed [CITE]. Understanding how virulent a pathogen can evolve before an epidemic begins can be helpful for controlling the disease. Furthermore, knowing the initial virulence, peak virulence, timing of the peak virulence, and equilibrium virulence provide sufficient detail to identify the shape of the virulence trajectory. During an epidemic outbreak, it is difficult to observe virulence evolution. Specifically,

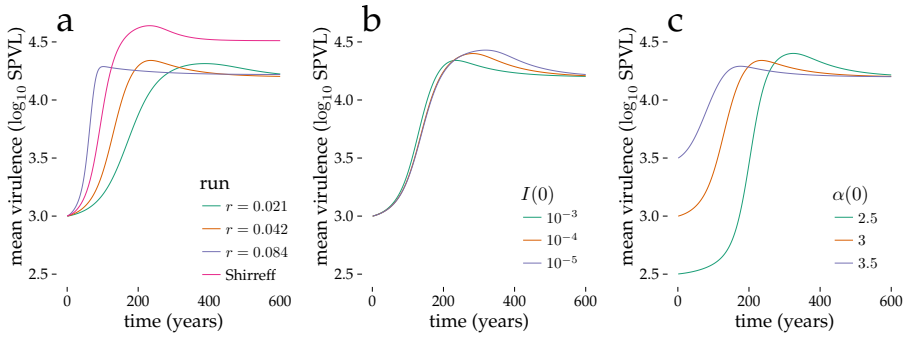

Figure 1: Baseline dynamics. Time series of mean population virulence ($\log_{10}$ SPVL). (a) Shirreff model, effects of varying r. (b) Effects of varying initial infectious density $I(0)$. (c) Effects of varying initial mean virulence $\alpha(0)$

in the case of HIV and other sexually transmitted diseases, slow evolutionary time-scale makes observing changes in the mean virulence even more challenging. Knowing the ranges of these statistics can help real-time virulence evolution prediction during an epidemic less troublesome.

3 Results

Our simplifications of Shirreff et al.'s model reproduce its qualitative behaviour reasonably well; as r decreases from 0.084 to 0.42 (the latter value matching the initial rate of increase in prevalence in Shirreff et al.'s full model) the initial trajectory of increasing virulence brackets the rate from the original model (Figure 1a). However, our model produces lower peak virulence ($\approx$? vs. $\approx$?) and equilibrium virulence $\approx$? vs. $\approx$?) than Shirreff's, even for matching initial incidence (i.e., $r = 0.042$).

Changing the initial infectious density ($I(0)$), while it produces the expected changes in the initial epidemic trajectory (Supplementary material), has little effect on the virulence trajectory, making the virulence peaks slightly later and larger as $I(0)$ decreases and allows a longer epidemic phase before the transition to endemic dynamics (Figure 1b). Decreasing the initial virulence similarly but more strongly leads to progressively later, larger peaks in virulence (Figure 1c).

Across the entire range of parameters covered by the LHS analysis, all of the classes of models we considered produce qualitatively similar virulence trajectories (Figure 2). Although the speed of virulence evolution varies, leading to wide variation in the peak virulence (means ranging from approximately 3.75 to 4.5 $\log_{10}$ SPVL), virulence peaks in all models between 200 and 300 years.

note that in Fig 1 we're using Shirreff's parameters

add Shir. params to table 1: Beta1=2.76, Dur1 = 0.25, Beta3 = 0.76, Dur3 = 0.75, c = 1.25, alpha={2,7,0.1}

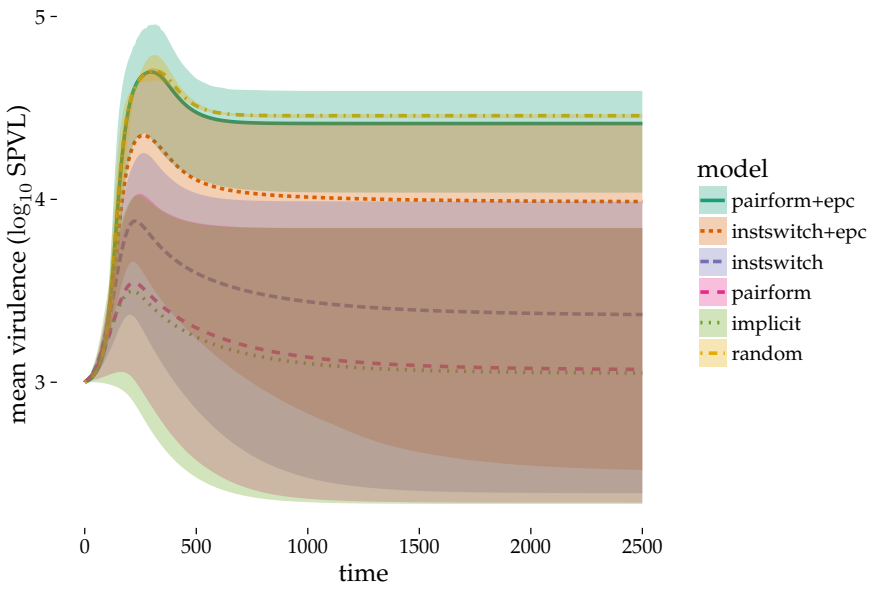

Figure 2: Envelopes of virulence trajectories under all models

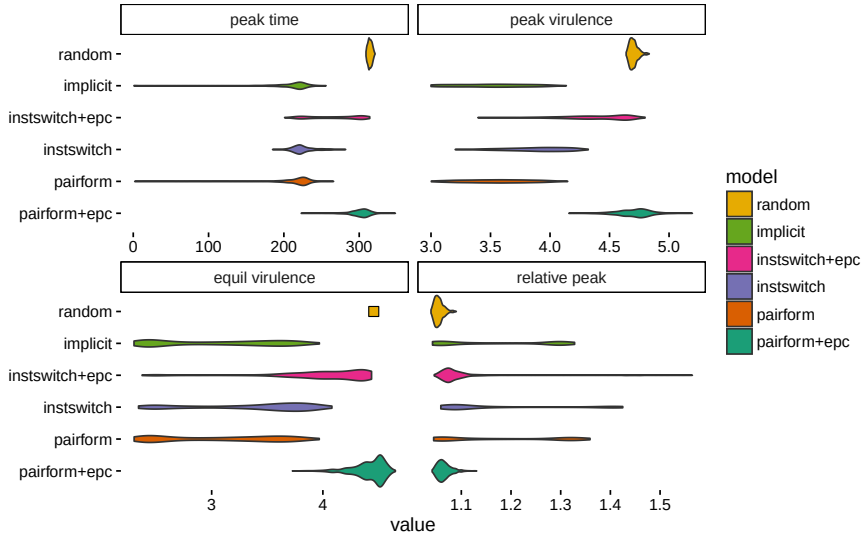

Figure 3: Univariate distributions of summary statistics. Note: point for eqvir/random is a placeholder, will have to be explained

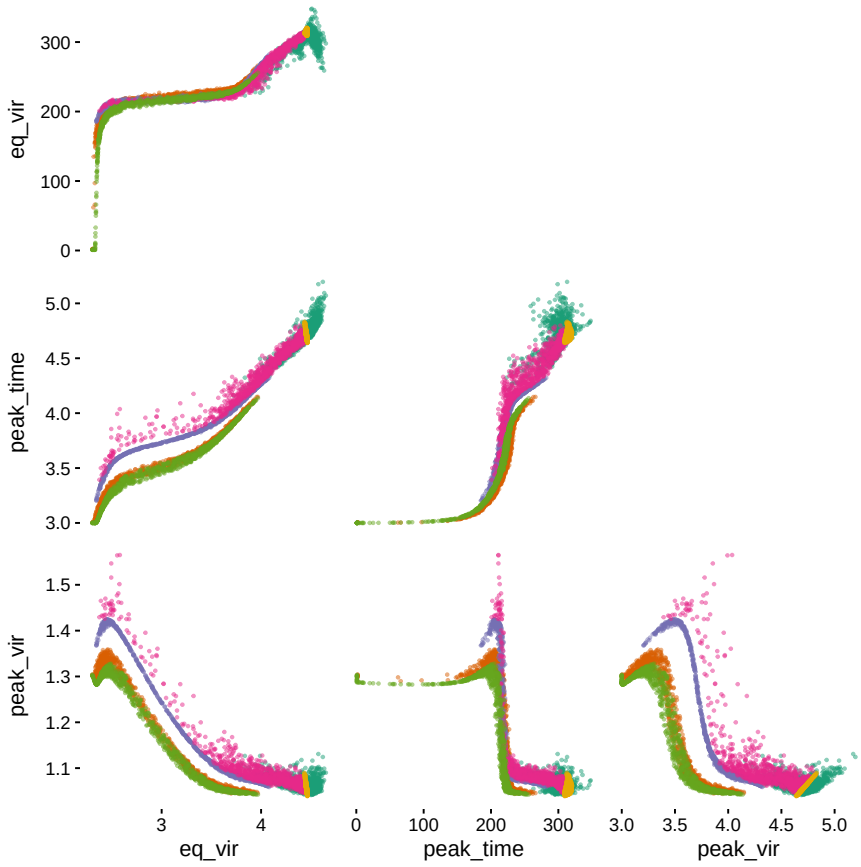

Figure 4: pairs plot

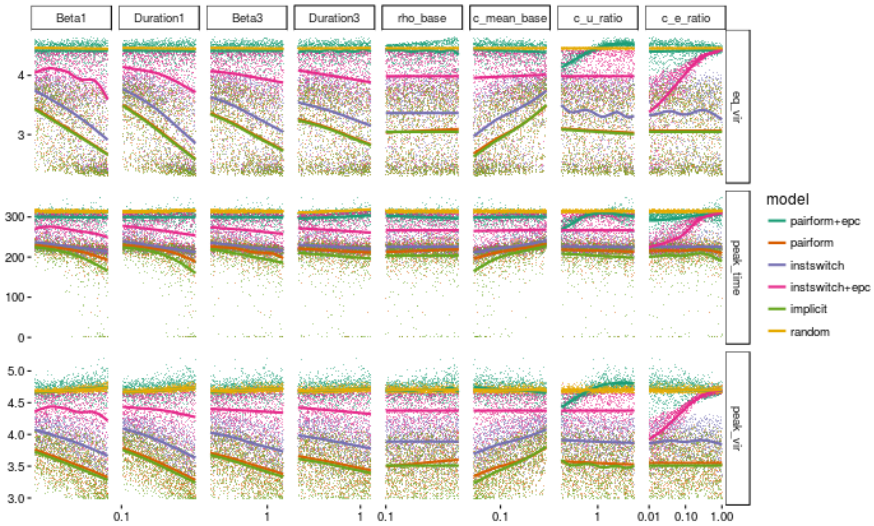

Figure to-do:

- fig 1. tweak size? remove redundant y axes/labels?
- fig 2. remove x-axis label; rename factor to make strip labels prettier. Log scale?
- fig 3.
- fig 4. pairs plot; legend?
- fig 5. sensitivity plot (unscaled plot); take out plots that are not related ... implicit model doesn't use rho, cu or ce; random doesn't use rho, cmean?, cu, ce; instswitch doesn't have rho or cu or ce; models without epc don't have ce or cu; instswitch + epc doesn't have rho and cu (no uncoupled compartment)

4 Discussion

5 To do

- clean up code and results
- incorporate pictures
- finish writing!
- hard parts of the results
  - explaining similarities among the models: why does implicit look most like pair formation model? (see R0comparison HTML)

- explaining sensitivity plot

See Bolker JRSI Google scholar cites (alternative link)

A Model details

Since we use multi-strain models, in which the distribution of $\log_{10}$ SPVL has been discretized into a vector, we use a matrix notation to describe our models. Five states described in the method section is replaced with the following notations: S, I_i, SS, SI_i, II_{ij}. Subscript indicates a strain that an individual is infected with. For example, I_i is number of infected individuals with $\log_{10}$ SPVL of α_i, and II_{ij} is the number of concordant couples, in which two partners have $\log_{10}$ SPVL of α_i and α_j. II_{ij} is equivalent to II_{ji}. Lastly, we define Kronecker delta as follows:

$$\delta_{ij} = \begin{matrix} 0 & \text{if} & i \neq j, \\ 1 & \text{if} & i = j. \end{matrix} \tag{7}$$

In our models, we introduce a non-standard use of Kronecker delta as exponent, such as $2^{\delta_{ij}}$. In a single-strain model, both individuals in a concordant partnership, II, enter single-infected compartment, I, when a partnership dissolves: $I' = 2cII'$. However, this is not the case in a multi-strain model. If infected individuals in an II partnership have different strains, they will enter different compartment. On the other hand, if both partners in an II partnership are infected with same strains, both will enter the same compartment. Therefore, we use Kronecker delta as exponent to distinguish such difference. Further details are explain below.

explain non-standard use of Kronecker delta as exponent!

Model 1 and 2 - Partnership dynamic

Single individuals acquire partners at rate ρ: $S' = -\rho S$ and $I_i' = -\rho I_i$. We follow Champredon et al's results and assume that single individuals are distributed into couple states through binomial distribution:

$$\begin{aligned} SS' &= \frac{\rho S \cdot S}{2(S + \sum_k I_k)} \\ SI_i' &= \frac{\rho S \cdot I_i}{S + \sum_k I_k} \\ II_{ij}' &= (\frac{1}{2})^{\delta_{ij}} \cdot \frac{\rho I_i \cdot I_j}{S + \sum_k I_k} \end{aligned} \tag{8}$$

We introduce Kronecker delta above to differentiate the partnership formation rate for II_{ij} when $i = j$ from that of $I \neq j$. When $i = j$ — like the partnership formation rate of SS — partnership formation rate becomes $II_{ii}' = \frac{\rho I_i \cdot I_i}{2(S + \sum_k I_k)}$

due to binomial distribution. On the other hand, when $i \neq j$, partnership formation rate becomes $II'_{ij} = \frac{\rho I_i I_j}{S+\sum_k I_k}$.

Partnerships dissolve at rate c: $SS' = -cSS$, $SI'_i = -cSI_i$, and $II_{ij} = -cII_{ij}$. Unlike single strain model, where both individuals leaving the II partnership would enter I, we have to account for strains which the individuals in concordant partnership are infected with (i.e. both partners in II_{ii} enter I_i whereas only one partner in II_{ij} enter I_i).

$$\begin{aligned} S' &= 2cSS + \sum_k cSI_k \\ I'_i &= cSI_i + \sum_k 2^{\delta_{ik}} cII_{ik} \end{aligned} \tag{9}$$

Combining partnership formation and dissolution process yields the following equation:

$$\begin{aligned} S' &= -\rho S + 2cSS + \sum_k cSI_k \\ I'_i &= -\rho I_i + cSI_i + \sum_k 2^{\delta_{ik}} cII_{ik} \\ SS' &= \frac{\rho S \cdot S}{2(S+\sum_k I_k)} - cSS \\ SI'_i &= \frac{\rho S \cdot I_i}{S+\sum_k I_k} - cSI_i \\ II'_{ij} &= (\frac{1}{2})^{\delta_{ij}} \cdot \frac{\rho I_i \cdot I_j}{S+\sum_k I_k} - cII_{ij} \end{aligned} \tag{10}$$

Model 1 and 2 - Infection

Within-couple transmission occurs in both models. An infected partner in SI partnership transmits virus to a susceptible partner, and partnership state becomes II: $SI'_i = -\beta_i SI_i$. Since we assume that mutation occurs, II_{ij}, where $i \neq j$, can be formed from both SI_i and SI_j partnership: $II'_{ij} = M_{ij}\beta_i SI_i + M_{ji}\beta_j SI_j$. On the other hand, II_{ii} can only be formed from an SI_i partnership: $II'_{ii} = M_{ii}\beta_i SI_i$. Using the Kronecker delta notation, we obtain following set of equations that describe within-couple transmission dynamics:

$$\begin{aligned} SI'_i &= -\beta_i SI_i \\ II_{ij} &= (\frac{1}{2})^{\delta_{ij}} \cdot (M_{ij}\beta_i SI_i + M_{ji}\beta_j SI_j) \end{aligned} \tag{11}$$

Champredon et al define the proportion of infectious extra-couple and uncoupled contact through the following term:

$$P = \frac{c_u I + c_e(SI + 2II)}{c_u(S+I) + 2c_e(SS + SI + II)}. \tag{12}$$

Effective uncoupled, c_u, and extra couple, c_e, contact rate can be divided into two terms: uncoupled/extra-couple contact rate $\times$ rate of transmission per contact. Therefore, transmission rate per contact term in c_u and c_e is canceled out in the equation above. Using this property, we modify the equation above as follows:

$$P = \frac{r_u I + r_e(SI + 2II)}{r_u(S + I) + 2r_e(SS + SI + II)}, \tag{13}$$

where $r_u = c_u/c_w$ and $r_e = c_e/c_w$ are the relative uncoupled/extra-couple contact rates. This simplification is useful in a multi-strain model since we cannot multiply a vector with a single value (e.g. $c_u S$ in denominator) if we use Champredon et al's equation as it is. Extending the above equation to multi-strain model so that P_i represents the proportion of the extra-couple and uncoupled contact of an infected individual with strain i, we obtain the following equation:

$$P_i = \frac{r_u I_i + r_e(SI_i + \sum_k (II_{ik} + \delta_{ik} II_{ik}))}{r_u(S + \sum_k I_k) + r_e(2SS + \sum_k 2SI_k + \sum_l \sum_k (1 + \delta_{lk}) II_{lk})}, \tag{14}$$

Using the equation above, we can model uncoupled and extra-couple mixing. For convenience, uncoupled and extra-couple transmission rates, c_u and c_e, will be replaced with $U_i = r_u \beta_i$ and $E_i = r_e \beta_i$ from now on.

Single susceptible individuals become infected and enter single infected compartment at the total rate of $\sum_k P_k U_k S$. Through mutation, newly infected individuals are distributed into each single infected compartments with different strains: $I_i' = \sum_k M_{ki} P_k U_k S$. Either partners in SS partnership can be infected and the partnership state can become SI partnership at the total rate of $\sum_i 2P_i E_i SS$. Formation of SI_i partnership is similar to the process through which single susceptible individuals are distributed into single infected compartments: $SI_i' = \sum_k 2M_{ki} P_k E_k SS$. Lastly, susceptible partner of an SI partnership can be infected due to uncoupled/extra-couple contacts and partnership can move to an II partnership. Like previous cases, SI_i partnership moves out of the compartment at a rate of $\sum_k P_k E_k SI_i$. Mutation process is similar to that of within-couple transmission. The only difference is that the $\log_1 0$ SPVL of a newly infected partner is not determined by its original partner but from an extra couple partner (i.e. the term P_i): $II_{ij}' = (1 - \frac{\delta_{ij}}{2})(\sum_k (M_{kj} P_k E_k SI_i + M_{ki} P_k E_k SI_j))$. Combining these equations we get the following set of equations that describe all the transmission dynamics

Model 1 and 2 - Disease induced mortality

Disease induced death rate, λ, is given by taking the reciprocate of the total duration of the infection: $\lambda_i = 1/(D_A + D_P(\alpha_i) + D_D)$. Since we assume SIS formulation, where infected individuals that die from infection enter single susceptible compartment, we obtain the following equation for the single infected individuals:

$$\begin{aligned} S' &= \sum_k \lambda_k I_k \\ I_i &= -\lambda_i I_i \end{aligned} \tag{15}$$

If an infected individual in a partnership dies, partnership dissolves. Thus, an SI_i partnership dissolves at a rate $-\lambda_i$, and the susceptible partner enters single susceptible compartment at rate $\lambda_i SI_i$ (infected partner that dies enter single susceptible compartment at an equal rate as well due to SIS formation):

$$\begin{aligned} S' &= \sum_k 2\lambda_k SI_k \\ SI_i &= -\lambda_i SI_i \end{aligned} \tag{16}$$

Similarly, II_{ij} partnership dissolves at a rate $-(\lambda_i + \lambda_j)$, but two cases, when $i \neq j$ and $i = j$, must be considered separately. When an II_{ij} partnership dissolves due to disease induced mortality, where $i \neq j$, death of partner with strain i causes its partner to enter I_j compartment at rate $\lambda_j II_{ij}$, and vice versa. When an $II_i i$ partnership dissolves, death of either partner causes the other partner to enter I_i compartment at rate $\lambda_i II_{ii}$, which sums up to $2\lambda_i II_{ii}$. Combining these dynamics yield the following equation:

$$\begin{aligned} S' &= \sum_l \sum_k 2^{\delta_{lk}} \lambda_k II_{lk} \\ I_i' &= \sum_k 2^{\delta_{ik}} \lambda_k II_{ik} \\ II_{ij}' &= -(\lambda_i + \lambda_j) II_{ij} \end{aligned} \tag{17}$$

Finally, combining all these equations give us the full model, which is model 1. We can simply take out the uncoupled and extra couple transmission term to obtain equation 2:

$$
\begin{aligned}
S' =& -\rho S + 2cSS + \sum_k cSI_k - \sum_k P_k U_k S + \sum_k \lambda_k I_k \\
&+ \sum_k 2\lambda_k SI_k + \sum_l \sum_k 2^{\delta_{lk}} \lambda_k II_{lk} \\
I_i' =& -\rho I_i + cSI_i + \sum_k 2^{\delta_{ik}} cII_{ik} + \sum_k M_{ki} P_k U_k S - \lambda_i I_i \\
&+ \sum_k 2^{\delta_{ik}} \lambda_k II_{ik} \\
SS' =& \frac{\rho S \cdot S}{2(S + \sum_k I_k)} - cSS - \sum_i 2P_i E_i SS \\
SI_i' =& \frac{\rho S \cdot I_i}{S + \sum_k I_k} - cSI_i - \beta_i SI_i + \sum_k 2M_{ki} P_k E_k SS - \sum_k P_k E_k SI_i \\
&- \lambda_i SI_i \\
II_{ij}' =& (\frac{1}{2})^{\delta_{ij}} \cdot \frac{\rho I_i \cdot I_j}{(S + \sum_k I_k)} - cII_{ij} + (\frac{1}{2})^{\delta_{ij}} \cdot (M_{ij}\beta_i SI_i + M_{ji}\beta_j SI_j) \\
&+ (\frac{1}{2})^{\delta_{ij}} \cdot (\sum_k (M_{kj} P_k E_k SI_i + M_{ki} P_k E_k SI_j)) - (\lambda_i + \lambda_j) II_{ij}
\end{aligned}
\tag{18}
$$

Model 3 and 4 - Partnership dynamic

Since model 3 and 4 assume instantaneous partnership formation, there are only three states: SS, SI_i, and II_{ij}. Partnership dissolution is equal to that of model 1 and 2: $SS' = -cSS$, $SI_i' = -cSI_i$, and $II_{ij}' = -II_{ij}$. Once the individuals leave partnership, they enter temporary compartments and are distributed into a partnership through binomial distribution:

$$
\begin{aligned}
X &= 2cSS + \sum_k cSI_k \\
Y_i &= cSI_i + \sum_k 2^{\delta_{ik}} cII_{ik} \\
SS' &= -cSS + \frac{X^2}{2(X + \sum_k Y_k)} \\
SI_i' &= -cSI_i + \frac{XY_i}{X + \sum_k Y_k} \\
II_{ij}' &= -cII_{ij} + (\frac{1}{2})^{\delta_{ij}} \frac{Y_i Y_j}{X + \sum_k Y_k}.
\end{aligned}
\tag{19}
$$

Model 3 and 4 - Infection

Model 3 and 4 share the within-couple transmission term with model 1 and 2. Since there is no single state, only extra couple transmission exists:

$$P_i = \frac{r_e(SI_i + \sum_k (II_{ik} + \delta_{ik} II_{ik}))}{r_e(2SS + \sum_k 2SI_k + \sum_l \sum_k (II_{lk} + \delta_{kl} II_{lk}))}. \tag{20}$$

Movement from SS state to SI state and SI to SS is modeled through the same equation that is used in model 1 and 2.

Model 3 and 4 - Disease induced mortality

Disease induced mortality is modeled similar to model 1 and 2. However, as single state does not exist in model 3 and 4, individuals that has left their partnerships due to death of their partners enter temporary compartments and form partners instantly:

$$\begin{aligned} X &= \sum_k 2\lambda_k SI_k + \sum_l \sum_k 2^{\delta_{lk}} \lambda_k II_{lk} \\ Y_i &= \sum_k 2^{\delta_{ik}} \lambda_k II_{ik} \\ SS &= = \frac{X^2}{2(X + \sum_k Y_k)} \\ SI_i &= -\lambda_i SI_i + \frac{XY_i}{X + \sum_k Y_k} \\ II'_{ij} &= -(\lambda_i + \lambda_j) II_{ij} + (\frac{1}{2})^{\delta_{ij}} \cdot \frac{Y_i Y_j}{X + \sum_k Y_k} \end{aligned} \tag{21}$$

Combining all these dynamics, we have equation 3. If we remove extra-couple transmission, we have equation 4.

$$\begin{aligned} X =& 2cSS + \sum_k cSI_k + \sum_k 2\lambda_k SI_k + \sum_l \sum_k 2^{\delta_{lk}} \lambda_k II_{lk} \\ Y_i =& cSI_i + \sum_k 2^{\delta_{ik}} cII_{ik} + \sum_k 2^{\delta_{ik}} \lambda_k II_{ik} \\ SS =& - cSS + \frac{X^2}{2(X + \sum_k Y_k)} - \sum_i 2P_i E_i SS \\ SI_i =& - cSI_i + \frac{XY_i}{X + \sum_k Y_k} - \beta_i SI_i + \sum_k 2M_{ki} P_k E_k SS \\ & - \sum_k P_k E_k SI_i - \lambda_i SI_i \\ II_{ij} & - cII_{ij} + (\frac{1}{2})^{\delta_{ij}} \frac{Y_i Y_j}{X + \sum_k Y_k} + (\frac{1}{2})^{\delta_{ij}} \cdot (M_{ij} \beta_i SI_i + M_{ji} \beta_j SI_j) \\ & + (\frac{1}{2})^{\delta_{ij}} \cdot (\sum_k (M_{kj} P_k E_k SI_i + M_{ki} P_k E_k SI_j)) - (\lambda_i + \lambda_j) II_{ij} \end{aligned} \tag{22}$$

Model 5

Model 5 is an implicit instantaneous partnership formation model, which uses adjusted transmission rate, β', that is derived from Hollingsworth et al's approximated basic reproduction number:

$$\beta_i' = \frac{c\beta_i}{c + \beta_i + \lambda_i}. \tag{23}$$

Thus, we get the following model:

$$\begin{aligned} S' &= \sum_k \lambda_k I_k - \sum_k \beta_k' S I_k \\ I_i &= \sum_k M_{ki} \beta_k' S I_k - \lambda_i I_i \end{aligned} \tag{24}$$

Model 6

Model 6 is a random mixing model. It is modeled in a same way as model 6 without the adjusted transmission rate:

$$\begin{aligned} S' &= \sum_k \lambda_k I_k - \sum_k \beta_k S I_k \\ I_i &= \sum_k M_{ki} \beta_k S I_k - \lambda_i I_i \end{aligned} \tag{25}$$

Initial distribution of infected individuals

We follow Champredon et al's result to calculate the initial distribution of infected individuals. For model 1 and 2, we have disease equilibrium state of $S^* = \frac{c}{c+\rho}$ and $SS^* = \frac{1-S^*}{2}$. We let $\epsilon = 10^{-4}$, which is the total number of infected individuals in the beginning of simulation and D be the vector such that D_i represent the proportion of individuals with $\log_{10}$ SPVL of i. Y_i is taken from normal distribution with mean 3 and is normalized so that $\sum_i D_i = 1$. Then, we have the following initial distribution of each states:

$$\begin{aligned} S(0) &= (1-\epsilon)S^* \\ SS(0) &= (1-\epsilon)^2 SS^* \\ SI_i(0) &= 2\epsilon(1-\epsilon)SS^* D_i \\ I_i(0) &= \epsilon S^* D_i \\ II_{ij}(0) &= (\frac{1}{2})^{\delta_{ij}} 2\epsilon^2 SS^* D_i D_j. \end{aligned} \tag{26}$$

Since model 3 and 4 do not have single state, $SS^* = 1$ at the disease free equilibrium and the initial distribution becomes as follows:

$$
\begin{aligned}
SS(0) &= (1-\epsilon)^2 SS^* \\
SI_i(0) &= 2\epsilon(1-\epsilon) SS^* D_i \\
II_{ij}(0) &= (\frac{1}{2})^{\delta_{ij}} 2\epsilon^2 SS^* D_i D_j .
\end{aligned}
\tag{27}
$$

Lastly, as model 5 is an implicit model, which does not consider different stages of partnership, we have the following initial distribution.

$$
\begin{aligned}
S(0) &= 1-\epsilon \\
I_i(0) &= \epsilon D_i .
\end{aligned}
\tag{28}
$$

Model 6 also shares the same distribution of initial infected individuals as model 5.

References

Alizon, S. (2009, May). The Price equation framework to study disease within-host evolution. *Journal of Evolutionary Biology 22*(5), 1123–1132.

Alizon, S. and Y. Michalakis (2015, January). Adaptive virulence evolution: the good old fitness-based approach. *Trends in Ecology & Evolution 30*(5), 248–254.

Blower, S. M., D. Hartel, H. Dowlatabadi, R. M. Anderson, and R. M. May (1991, February). Drugs, sex and HIV: A mathematical model for New York City. *Philosophical Transactions of the Royal Society of London B: Biological Sciences 331*(1260), 171–187.

Champredon, D., S. Bellan, and J. Dushoff (2013, 12). HIV sexual transmission is predominantly driven by single individuals rather than discordant couples: A model-based approach. *PLoS ONE 8*(12), e82906.

Day, T. and S. R. Proulx (2004, April). A general theory for the evolutionary dynamics of virulence. *The American Naturalist 163*(4), E40–E63.

Dwyer, G., S. Levin, and L. Buttel (1990). A simulation model of the population dynamics and evolution of myxomatosis. *Ecol Monog 60*, 423–447.

Ebert, D. (1999). The evolution and expression of parasite virulence. In S. C. Stearns (Ed.), *Evolution in Health & Disease*, Chapter 14, pp. 161–172. New York: Oxford University Press, Oxford, UK.

Ebert, D. and J. J. Bull (2003). Challenging the trade-off model for the evolution of virulence: is virulence management feasible? *Trends Microbiol 11*(1), 15–20.

Fraser, C., T. D. Hollingsworth, R. Chapman, F. de Wolf, and W. P. Hanage (2007). Variation in HIV-1 set-point viral load: Epidemiological analysis and an evolutionary hypothesis. *PNAS 104*, 17441–17446.

Fraser, C., K. Lythgoe, G. E. Leventhal, G. Shirreff, T. D. Hollingsworth, S. Alizon, and S. Bonhoeffer (2014, March). Virulence and Pathogenesis of HIV-1 Infection: An Evolutionary Perspective. *Science 343*(6177), 1243727.

Herbeck, J. T., J. E. Mittler, G. S. Gottlieb, and J. I. Mullins (2014, June). An HIV epidemic model based on viral load dynamics: Value in assessing empirical trends in HIV virulence and community viral load. *PLoS Comput Biol 10*(6), e1003673.

Herbeck, J. T., V. Mller, B. S. Maust, B. Ledergerber, C. Torti, S. Di Giambenedetto, L. Gras, H. F. Gnthard, L. P. Jacobson, J. I. Mullins, and G. S. Gottlieb (2012, January). Is the virulence of HIV changing? A meta-analysis of trends in prognostic markers of HIV disease progression and transmission. *AIDS (London, England) 26*(2), 193–205.

Hollingsworth, T., R. Anderson, and C. Fraser (2008, September). HIV-1 Transmission, by Stage of Infection. *Journal of Infectious Diseases 198*(5), 687–693.

Payne, R., M. Muenchhoff, J. Mann, H. E. Roberts, P. Matthews, E. Adland, A. Hempenstall, K.-H. Huang, M. Brockman, Z. Brumme, M. Sinclair, T. Miura, J. Frater, M. Essex, R. Shapiro, B. D. Walker, T. Ndungu, A. R. McLean, J. M. Carlson, and P. J. R. Goulder (2014, December). Impact of HLA-driven HIV adaptation on virulence in populations of high HIV seroprevalence. *Proceedings of the National Academy of Sciences 111*(50), E5393–E5400.

Shirreff, G., L. Pellis, O. Laeyendecker, and C. Fraser (2011, October). Transmission selects for HIV-1 strains of intermediate virulence: A modelling approach. *PLoS Computational Biology 7*(10), e1002185. WOS:000297262700019.

Table 1: Parameter ranges/values

Notation	Description	Range/Value	Source
ρ	Partnership formation rate	1/10-2/5	Champredon et al. (2013)
c	Partnership dissolution rate	1/15-1/5	Champredon et al. (2013)
c_u/c_w	Relative contact rate uncoupled	1/5-5	Assumption
c_e/c_w	Relative contact rate extra-couple	0.01-1	Champredon et al. (2013)
β_P	Rate of transmission during primary infection	1.31-5.09	Hollingsworth et al. (2008)
β_D	Rate of transmission during high transmission disease stage	0.413-1.28	Hollingsworth et al. (2008)
D_P	Duration of primary infection	1.23/12-6/12	Hollingsworth et al. (2008)
D_D	Duration of high transmission disease stage	4.81/12-14/12	Hollingsworth et al. (2008)
β_{max}	Maximum rate of transmission during asymptomatic stage	0.317	Shirreff et al. (2011)
β_{50}	SPVL at which infectiousness is half maximum	13938	Shirreff et al. (2011)
β_k	Hill coefficient: steepness of increase in infectiousness as a function of SPVL	1.02	Shirreff et al. (2011)
D_{max}	Duration of primary infection	25.4	Shirreff et al. (2011)
D_{50}	SPVL at which duration of asymptomatic infection is half maximum	3058	Shirreff et al. (2011)
D_k	Hill coefficient: steepness of decrease in duration as a function of SPVL	0.41	Shirreff et al. (2011)
σ_M	Mutation standard deviation of $\log_{10}$ SPVL	0.12	Shirreff et al. (2011)
α_{min}	Minimum $\log_{10}$ SPVL	2	Shirreff et al. (2011)
α_{max}	Maximum $\log_{10}$ SPVL	2	Shirreff et al. (2011)
n	Number of strains	21	Assumption